Electrical properties of undoped $Ga_xIn_{1-x}P$/GaAs quantum wells

Said Elhamri, M. Ahoujja, R. S. Newrock, D. B. Mast, and S. T. Herbert*
Department of Physics, University of Cincinnati, Cincinnati, Ohio 45221-0011

W. C. Mitchel
Wright Laboratory, Materials Directorate, Wright-Patterson Air Force Base, Ohio 45433-7707

Manijeh Razeghi
Center for Quantum Devices, Department of Electrical Engineering and Computer Science, Northwestern University, Evanston, Illinois 60208

(Received 4 April 1996)

We report a study of $Ga_xIn_{1-x}P$/GaAs in very thin quantum wells. Our samples are not intentionally doped; nevertheless, we observed that exposing this structure to red light induces a photocurrent which is persistent at low temperatures. This is accompanied by an increase in the carrier concentration, the Hall mobility, and the quantum scattering time. Since the shallow donor concentration in the $Ga_xIn_{1-x}P$ layers is too low to produce the observed concentration, the persistent photocarriers cannot be produced by *DX*-like defects. We suggest that the persistent carriers are produced by photoionization of deep intrinsic donors in the $Ga_xIn_{1-x}P$ barrier layer. Extended illumination also induces a parallel conduction path. In the case of an infinite barrier height, theoretical studies predict that in thin quantum wells such as ours, interface roughness is the dominant low-temperature scattering mechanism and that the mobility in these wells should vary as L^6 where L is the well width. In the case of a finite barrier height, theoretical studies predict that the mobility will not depend as strongly on L. Our measured mobilities follow an $L^{1.3}$ dependence, resulting in higher mobilities and supporting what is predicted theoretically. As predicted, we believe that this dependence is due to the finite barrier height of the quantum well. The barrier height affects how much of the electron wave function penetrates into the barrier and hence influences how interface roughness scattering affects the mobility. [S0163-1829(96)09139-4]

I. INTRODUCTION

For more than a decade GaAs/$Al_xGa_{1-x}As$ has been the most widely studied heterostructure. Grown by molecular-beam epitaxy (MBE), it exhibits extremely high electron mobilities, which have proven to be very useful for both fundamental research and for applications in electronic devices.[1] However, this material has some very important drawbacks,[2–5] most noticeably the presence of deep defect levels (*DX* centers) and oxidation of the aluminum. The presence of *DX* centers[6,7] gives rise to the so-called persistent photoconductivity (PPC), which makes precise control and stability of the carrier concentration, required in electronic devices, very difficult. This can lead to an instability in the *IV* curves for field effect transistors (FET's) or *IV* ''collapse'' in the dark.[8] The oxidation of the aluminum gives rise to poor interfaces and can degrade the entire structure. $Al_xGa_{1-x}As$ is also sensitive to both oxygen and humidity. If present during growth, these contaminants can lead to high resistance and bad optical quality.[9] This is especially important when growing $Al_xGa_{1-x}As$ with metal-organic chemical-vapor deposition (MOCVD).

Because of these problems, there has been a search for an alternative to $Al_xGa_{1-x}As$. Recently the phosphorus-based alloy $Ga_xIn_{1-x}P$ has received considerable attention as an alternative to $Al_xGa_{1-x}As$. This is mainly due to the belief that the many problems involved with using aluminum will either be reduced or eliminated. $Ga_xIn_{1-x}P$, like $Al_xGa_{1-x}As$, is a III-V semiconductor compound and the interest in this material is justified when its *material* properties are compared to those of $Al_xGa_{1-x}As$.

When lattice matched to GaAs, $Ga_xIn_{1-x}P$ has a direct band gap of 1.9 eV, making it especially attractive for microwave devices as well as for optical devices operating in the visible region.[1] This band gap is as large as that of $Al_xGa_{1-x}As$ containing about 40% aluminum, an amount usually avoided because it puts the band gap very close to where the material makes the transition from a direct to an indirect band gap.

A second advantage of $Ga_xIn_{1-x}P$ is that the $Ga_xIn_{1-x}P$/GaAs interface exhibits a low surface recombination velocity,[10–12] about 1.5 cm/sec, nearly two orders of magnitude smaller than that of a typical $Al_xGa_{1-x}As$/GaAs interface.[13] This makes this material combination attractive for use in high-speed applications, such as in high electron mobility transistors, where small values of the surface recombination velocity lead to a reduction in the low-frequency noise of the device.[2] Also, compared to $Al_xGa_{1-x}As$, $Ga_xIn_{1-x}P$ has a high doping efficiency. That is, for the same amount of dopant concentration in both $Ga_xIn_{1-x}P$ and $Al_xGa_{1-x}As$, a higher two-dimensional electron gas (2DEG) carrier density is obtained at the interface of $Ga_xIn_{1-x}P$/GaAs than at the interface of $Al_xGa_{1-x}As$/GaAs. This is because the donor energy levels in $Ga_xIn_{1-x}P$/GaAs are shallow. The difference in the energy-band discontinuity may also be responsible for this; however, this is a matter of

TABLE I. Structural schematic of the samples. None of the layers was intentionally doped.

Sample A	Sample B	Sample C	Sample D
2000-Å $Ga_xIn_{1-x}P$	300-Å $Ga_xIn_{1-x}P$	100-Å $Ga_xIn_{1-x}P$	100-Å $Ga_xIn_{1-x}P$
20-Å GaAs	25-Å GaAs	50-Å GaAs	75-Å GaAs
9000-Å GaInP	300-Å $Ga_xIn_{1-x}P$	5000-Å $Ga_xIn_{1-x}P$	5000-Å $Ga_xIn_{1-x}P$
5000-Å GaAs	25-Å GaAs	500-Å GaAs	500-Å GaAs
S.I. GaAs substrate	9000-Å $Ga_xIn_{1-x}P$	S.I. GaAs substrate	S.I. GaAs substrate
	5000-Å GaAs		
	semi-insulating GaAs substrate		

some debate. Some authors estimated the conduction-band discontinuity at the $Ga_{0.52}In_{0.48}P$/GaAs interface to be 0.4 eV (Ref. 14) (larger than that at the $Al_{0.3}Ga_{0.7}As$/GaAs interface) while others estimated the conduction-band discontinuity to be less than 0.2 eV.[15,16]

It is believed that the 2DEG formed at the $Ga_xIn_{1-x}P$/GaAs interface has electrical properties superior to those of the one in $Al_xGa_{1-x}As$/GaAs.[17–19] This is because the location of the direct-indirect conduction-band crossover is at $x=0.74$ for $Ga_xIn_{1-x}P$, while the location for lattice matching to GaAs is some distance away from it at $x=0.51-0.52$. Consequently, only a few *DX* centers may exist in this material compared to $Al_xGa_{1-x}As$. This is one of the important things that motivated the study of heterostructures made of this material combination.

II. PERSISTENT PHOTOCONDUCTIVITY

Exposing certain heterostructures to light results in the ionization of defects in the barrier. The electrons freed from the defects migrate to the well which hosts the 2DEG, resulting in an increase in the conductivity of the channel. At low temperatures, this change in the conductivity is persistent for a long time [in some systems greater than 10^8 sec (Ref. 20)] because the extra electrons cannot recombine with the donors due to the existence of a capture barrier. This effect is known as positive persistent photoconductivity (PPC). In some samples, exposure to light results in a reduction of the conductivity, and at low enough temperatures this effect is also persistent. This is referred to as negative persistent photoconductivity (NPPC).

The PPC has been widely studied in $Al_xGa_{1-x}As$/GaAs heterostructures and it is now widely accepted that it has its origin in DX centers[21] associated with the doping level (for a compilation of the properties of this center see Ref. 21). The concentration of DX centers increases with doping and, depending on the aluminum concentration, the existence of DX centers may or may not result in PPC; for an aluminum concentration less than 0.20, DX centers do not give rise to PPC in $Al_xGa_{1-x}As$/GaAs structures.

It was originally thought that since $Ga_xIn_{1-x}P$/GaAs has no aluminum, there would be no PPC in this structure. However, there have been many reports of it in single $Ga_xIn_{1-x}P$/GaAs heterojunctions. Razeghi and co-workers[22,23] reported PPC in undoped single interface heterostructures grown by MOCVD, but left open the question of where the electrons come from. They reported a carrier concentration of 1.7×10^{11} cm^{-2} before illumination, increasing to about 4.1×10^{11} cm^{-2} after illumination. Razeghi and coworkers also reported one of the highest recorded mobilities in this material, $\mu=780\,000$ cm^2/V sec at liquid-helium temperatures. No spacer was used as this was an undoped structure. Paloura *et al.*,[13] in a study of metal-organic molecular-beam-epitaxy (MOMBE) -grown bulk films, reported the observation of PPC in undoped and S-doped samples, while in Si-doped samples the PPC was suppressed to insignificant levels. Using deep-level transient spectroscopy, they reported that the undoped layers are characterized by a deep electron trap with an activation energy that depends on the gallium mole fraction and takes values in the range 820 to 875 meV. However, when either S or Si doping is introduced, this trap center is suppressed and a new trap appears at 300–345 meV. Feng *et al.*,[24] in a capacitance-voltage and deep-level transient spectroscopy study of undoped bulk $Ga_xIn_{1-x}P$, reported the observation of two electron traps. The first, with a small concentration $\sim10^{13}$ cm^{-3}, is 75 meV below the conduction band. The second, with a concentration of $10^{14}-10^{15}$ cm^{-3}, is 0.9 eV below the conduction band and emits electrons above room temperature ($\sim$350 K). Ginoudi *et al.*[2] also reported the observation of PPC in S-doped $Ga_xIn_{1-x}P$/GaAs high electron mobility transistors grown by MOMBE, but point out that Si doping suppresses the PPC to insignificant amounts. They conclude that Si is a more suitable donor for low-temperature devices made of this material. On the other hand, Krynicki *et al.*[25] studied Si-doped $Ga_xIn_{1-x}P$ layers and report a PPC. Responsible for this PPC is a new defect, with an ionization energy of 0.435 eV, located only about 20 meV below the conduction band. The concentration of this defect increases with the doping concentration. For material with 1.18×10^9 cm^{-3} free carriers, they report a concentration of this new defect of 5×10^{17} cm^{-3}. They argue that the reason the defect present in the undoped structure is not observed in their work on doped samples is because its concentration is much smaller. Also worth noting is that the ionization energy reported for the defect in doped samples seems to depend not only on the nature of the dopant (0.31 and 0.37 eV are reported for Si and S doping, respectively[2]), but also on the experimental conditions.[26] It is clear from these somewhat conflicting reports that additional studies of this promising material are necessary to clarify what is producing the PPC. In this section, we discuss our Shubnikov–de Haas and low-field Hall effect studies of the PPC in undoped $Ga_xIn_{1-x}P$/GaAs *quan-*

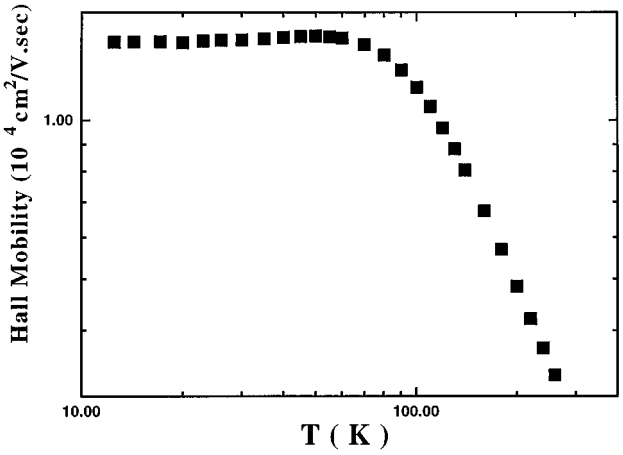

FIG. 1. The Hall mobility as function of temperature for sample *C* (the 50-Å well). The results are similar for all other samples. This mobility behavior as a function of temperature is a signature of a two-dimensional electron gas.

tum wells. Recall that the Shubnikov–de Haas effect is a particularly useful technique for the study of two-dimensional electron gases in heterostructures because of the wealth of information it provides on the carriers.

The samples in this study (see Table I) were grown by low-pressure metal-organic chemical-vapor deposition (LP-MOCVD), at a pressure of 76 Torr and a temperature of 510 °C on GaAs substrate orientated at 2° off (100). Trimethylindium and triethylgallium were used as sources of indium and gallium, and pure arsine (AH_3) and phosphine (PH_3) provided the arsenic and phosphorus, respectively. Hydrogen was used as the carrier gas. We have also confirmed that no ordering is present in the four separate wafers that were grown for this study. The first two wafers began with a 0.5-μm GaAs buffer layer grown on a semi-insulating GaAs substrate, followed by a 0.9-μm lattice-matched $Ga_{0.51}In_{0.49}P$ barrier. On the first wafer, a single 20-Å GaAs well, capped with 2000 Å of $Ga_xIn_{1-x}P$ was grown. On the second wafer, a double quantum well was formed by growing 25 Å of GaAs, 300 Å of $Ga_xIn_{1-x}P$, another 25 Å of GaAs, and, finally 300 Å of $Ga_xIn_{1-x}P$. The third and fourth wafers also began with a 0.05-μm GaAs buffer layer, grown on a semi-insulating GaAs substrate, followed by a 0.5-μm lattice-matched $Ga_{0.51}In_{0.49}P$ barrier. On the third wafer a single 50-Å well was grown and on the fourth a 75-Å well was grown. Both wafers were capped with 100 Å of undoped $Ga_xIn_{1-x}P$. All layers were undoped and all $Ga_xIn_{1-x}P$ layers had the same alloy concentration ($Ga_{0.51}In_{0.49}P$).

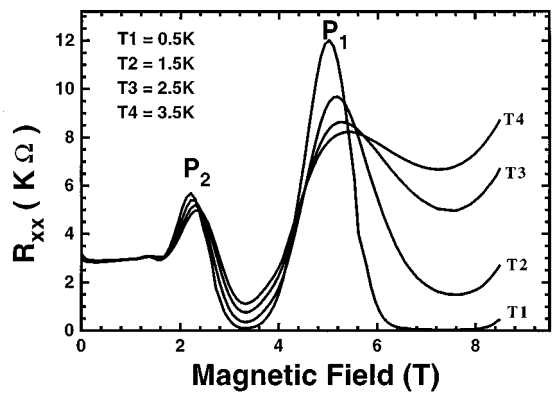

FIG. 2. R_{xx} as a function of temperature for sample *B*. P_1 and P_2 are labels for two of the peaks (see text).

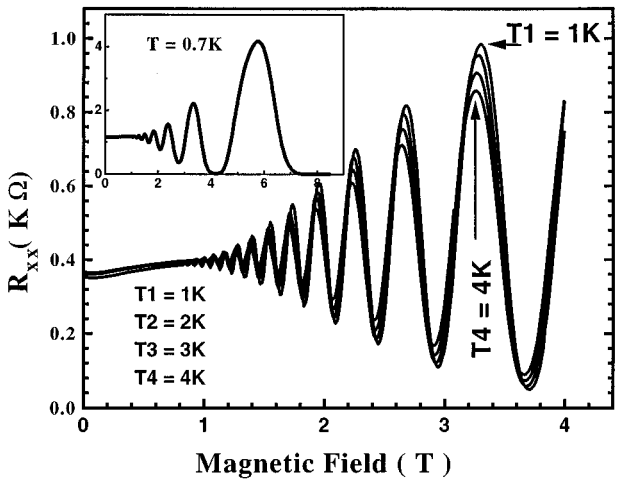

FIG. 3. The dependence of R_{xx} on T for sample *D* before illumination. The inset shows the behavior of R_{xx} at $T=0.7$ K over a wider field range. Notice that the R_{xx} minima become broad and approach zero at high fields.

Measurements were done on several samples from each of the four wafers, but as the results from samples from the same wafer were essentially identical, we detail only the measurements done on one sample from each wafer, labeled sample *A* (the first wafer), sample *B* (the second wafer), sample *C* (the third wafer), and sample *D* (the fourth wafer).

Figure 1 shows the behavior of the mobility μ as a function of the temperature T. This particular dependence of the mobility on temperature is one of the signatures of a 2DEG, and all our samples exhibit this behavior. The most important difference among the four samples is that sample *A* (20-Å well) did not conduct at or below 20 K. Figure 2 shows the Shubnikov–de Haas data for sample *B* (25-Å well) as a function of temperature. Note that at high fields R_{xx} goes to zero for $T=0.5$ K, but as the temperature increases the minima deviate from zero. This deviation is due to a thermal activation energy. In addition, the maxima appear to shift to higher fields as the temperature increases, indicating an apparent change in the carrier concentration with temperature. However, a close look at the peaks labeled P_1 and P_2 reveals both move to slightly higher fields as the temperature increases, but the period of the oscillation does not change. Since the period depends only on the carrier concentration, we conclude that the carrier density in the 2DEG is fixed over this temperature range.

Figure 3 shows, for sample *D* (75-Å well), the typical temperature dependence of the longitudinal resistance R_{xx} before illumination. The inset in the figure shows the behavior of R_{xx} for higher fields and from this inset we see that the minima in R_{xx} do go to zero as the field increases. The main difference between Figs. 2 and 3 is the number of oscillations observable in the 0–4-T field range. Sample *D* (Fig. 3) shows more oscillations because the carrier concentration is higher in this sample than in sample *B*. Before illumination, room-temperature Hall measurements indicated a carrier

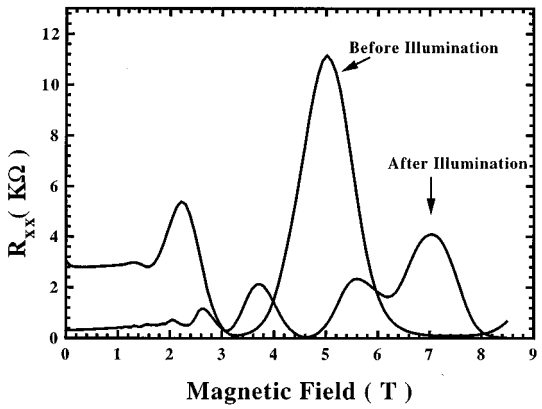

FIG. 4. R_{xx} before and after illumination for sample B.

concentration in the high 10^{10} cm^{-2} to low 10^{11} cm^{-2} for sample B (and also A), whereas for sample D (and also C) the carrier concentration is on the order of 4×10^{11} cm^{-2}.

To investigate the PPC, the samples were cooled to liquid-helium temperatures and both Hall and Shubnikov–de Haas measurements were carried out as a function of temperature. The results are shown in Figs. 4 and 5. Each sample was then illuminated with a red light- (~700 nm) emitting diode (LED) for several minutes. After the light was turned off, Shubnikov–de Haas and Hall measurements were performed. Figure 4 shows two curves, before and after illumination; both curves were taken in the dark (that is, the data for the second curve were taken after the LED was turned off). Figure 5 shows similar data for sample D. In general, we observed that the PPC was the same in all samples and we will only present results for sample B unless otherwise indicated.

It is worth noting in Figs. 4 and 5 that the minima of R_{xx} go to zero in the quantum Hall regime, indicating that all conduction is in the well, with no parallel conduction paths in the $Ga_xIn_{1-x}P$ barriers for this initial amount of illumination. If there had been additional conduction paths, they would have manifested themselves as a monotonously increasing background on the Shubnikov–de Haas oscillations, including the minima.

Exposing these heterostructures to light results in several changes. First, the zero-field resistivity decreases. Second, the number of oscillations in a given field range increases, indicating that the period of the oscillations has decreased.

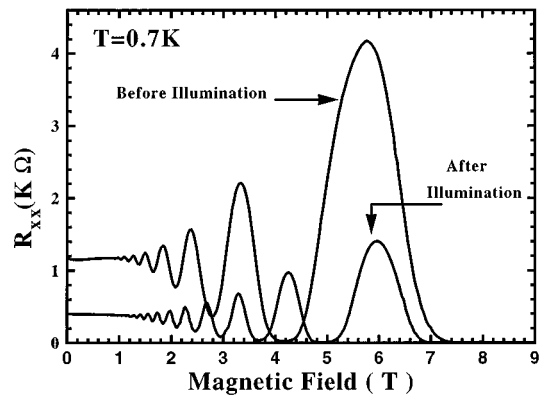

FIG. 5. R_{xx} before and after illumination for sample D.

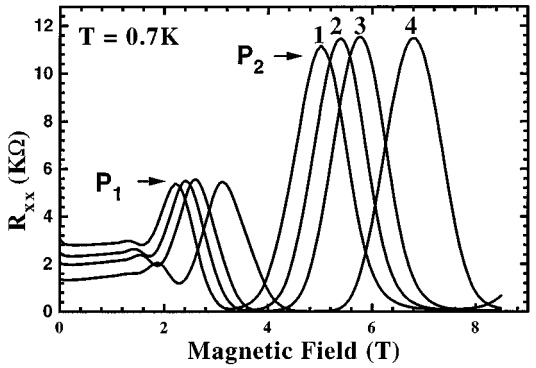

FIG. 6. Evolution of the Shubnikov–de Haas oscillations with a gradual illumination of the sample at 0.7 K. Peaks P_1 and P_2 are labeled on the unilluminated curve. As the illumination increases, the two peaks progressively shift to higher fields.

Third, the light appears to induce a large reduction in the amplitude of the oscillating resistance. The reduction in the zero-field resistivity and the decrease in the period of the oscillations, both of which are inversely proportional to the carrier density, are indicative of an increase in the carrier concentration due to the illumination.

The most obvious effect of illumination is the apparent reduction in the amplitude of the oscillations, a result indicative of a decrease in the quantum lifetime (this lifetime is a measure of the collision broadening of the Landau levels and is related to the half width of the broadened Landau level. The different scattering mechanisms that contribute to the broadening of the Landau levels determine the value of this lifetime), if the oscillations compared are from the same Landau level. In these samples, however, the increase in the carrier concentration due to the PPC fills more Landau levels and has the effect of shifting the oscillations to higher fields. Consequently, oscillations corresponding to the same set of Landau levels cannot be observed in the two curves of Fig. 4. To study the effects on the amplitudes of the resistance oscillations we used shorter illumination times, as short as 2 sec. We warmed up the samples to room temperature to rid it of the effect of the first illumination and then cooled down to 0.7 K. These results, along with the original dark curve, are shown in Fig. 6. Here the evolution of each oscillation can be followed as the carrier concentration increases with increasing illumination time. Curve 1 was obtained before illumination and the illumination time increases from curve 2 to 4 (to obtain the data, we illuminated the sample for 2 sec, turned off the light and gathered data for trace 2. The sample was then illuminated for an additional 2 sec and the data for trace 3 taken after turning off the light. Finally, the sample was illuminated for an additional 2 sec to gather data for the curve 4). As expected, the maxima and minima (see peaks P_1 and P_2 in Fig. 6) shift to higher fields, but the amplitudes of the oscillations, which originate from the same Landau levels, clearly *increase* and do *not decrease*. The amplitude of peak P_1, for example, increased by about 65%. This shows that the quantum lifetime increases after illumination. The increase in the amplitude of peak P_2 is not as dramatic, due to the presence of spin splitting, which also affects the amplitude of the oscillations. Another interesting result of the PPC, shown in Fig. 7, is the sharpening of the quantum

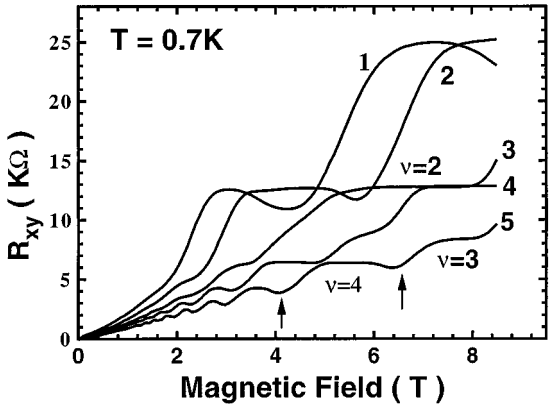

FIG. 7. R_{xy} for different illumination times, with the illumination time increasing from left to right. Curve 1 was taken before illumination. Curve 5 was taken after several illuminations. All data were taken in the dark. *These curves correspond to different illumination times than the ones shown in Fig. 6*. The arrows indicate dips in the quantum Hall plateaus where they deviate from the theoretical values.

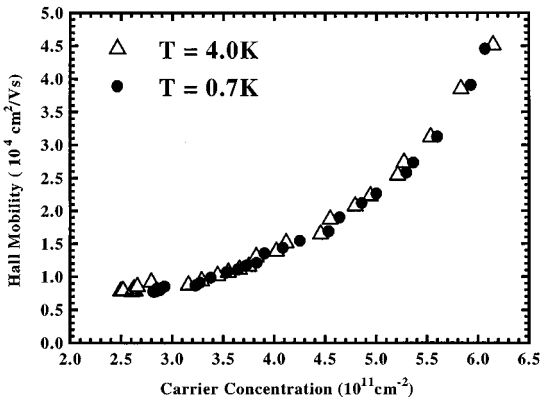

FIG. 8. The Hall mobility as a function of the Hall carrier concentration, for two different temperatures. We notice no significant temperature dependence of the mobility in this temperature range.

Hall effect. Curve 1 was taken before illumination and the others after each additional illumination. Curve 5 was taken after the sample was saturated (that is, we illuminated the sample for a sufficiently long time that additional exposure to light did not change the carrier concentration of the sample). Initially there is structure (curves 1 and 2) in the $n=2$ quantum Hall plateau, but as the total illumination time increases, this gradually disappears, leaving an unusually wide plateau (curve 3). The structure in curves 1 and 2 is normally indicative of a parallel conduction path, but the presence of such a conduction path would manifest itself as a monotonously *increasing* background in R_{xx} leading to deviations of the R_{xx} minima from zero. But, as we remarked above, from Fig. 4, the minima of R_{xx} (before illumination) are *decreasing* with magnetic field, are broad, and are approaching zero in the quantum Hall regime. The presence of this structure in the quantum Hall effect must have its origin in something other than parallel conduction paths. We believe it is a result of a nonuniform spatial distribution of the 2DEG, but do not yet have a convincing explanation.

Also observable in Fig. 7 is an apparent deviation after *extended* illumination of the plateau values from the theoretical quantized values (see curve 5 and the dips indicated by the arrows). This type of dip in the Hall plateaus *accompanied* by deviations of the R_{xx} minimum from zero are indicative of the presence of a parallel conduction path. To the best of our knowledge, parallel conduction induced by extended illumination was reported[27] for the first time by our group.

The PPC allows us to study the dependence of the mobility on the carrier concentration in a single sample. We have done this for our samples and the results for sample *B* are displayed in Fig. 8. The mobility depends strongly on the carrier concentration, increasing rather rapidly as a function of the carrier density. The dependence of the mobility on the carrier density is not sensitive to temperature between 0.7 and 4 K.

In summary, we found several effects due to the PPC. First, it enhances the carrier concentration, increasing it from about 9×10^{10} cm^{-2} to about 3×10^{11} cm^{-2} for sample *A*, from about 3×10^{11} cm^{-2} to about 7×10^{11} cm^{-2} for sample *B*, and from about 4×10^{11} cm^{-2} to about 9×10^{11} cm^{-2}, for samples *C* and *D*. Second, the PPC results in an increase in the Hall mobility and hence the classical scattering time. Third, the PPC also leads to an increase in the quantum scattering time, as reflected by the increase in the amplitude of the resistance oscillations corresponding to the same set of Landau levels.

The most interesting feature we observed in the PPC is that both the classical and the quantum lifetimes increase after illumination. An increase in either of these, after a photoinduced increase in carrier density, is rare.[28] In most measurements of lifetime changes in heterostructures and quantum wells, the scattering times decrease with increasing carrier concentration, due to an increase in the number of ionized defects from which the additional carriers were photoexcited.[28–30] An increase in scattering times, with a concomitant increase in carrier concentration, can only result from a decrease in the number of ionized defects or an increase in the screening of the defects. Since unintentionally doped $Ga_xIn_{1-x}P$ grown by MOCVD is *n* type, the only way to increase the electron concentration while reducing the ionized center concentration would be to photoexcite electrons trapped at compensating acceptors in the $Ga_xIn_{1-x}P$ barriers and have them transfer to the well before they are recaptured. This seems unlikely. Thus we believe an increase in screening is the most likely process for the increase in the low-field mobility and the quantum lifetime.[31]

The increase in the carrier concentration after illumination raises an important question: since these structures are not intentionally doped, what is the source of the extra electrons? If electrons from unintentionally introduced impurities are responsible for the increase in the carrier density after illumination, then the concentration of these background dopants has to be higher than 1×10^{17} cm^{-3}. This is very unlikely. With MOCVD fabrication processes the normal levels of unintentional dopants range from the high 10^{14} to 10^{15} cm^{-3}, two orders of magnitude too low. The source of these extra electrons is most likely the deep donors observed in undoped $Ga_xIn_{1-x}P$ and located 0.8–0.9 eV below the conduction band.[13,25] The question of whether or not this is a DX-like center remains open. For comparison purposes, we studied five undoped $Al_xGa_{1-x}As$/GaAs single quantum

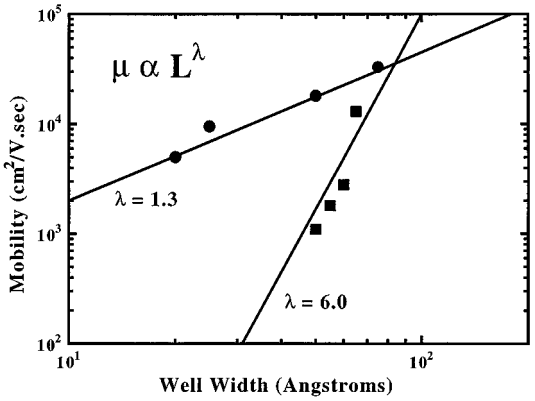

FIG. 9. The mobility as a function of the well width. The circles are our data. The squares are extrapolated data points from Fig. 1 of Sakaki *et al.*

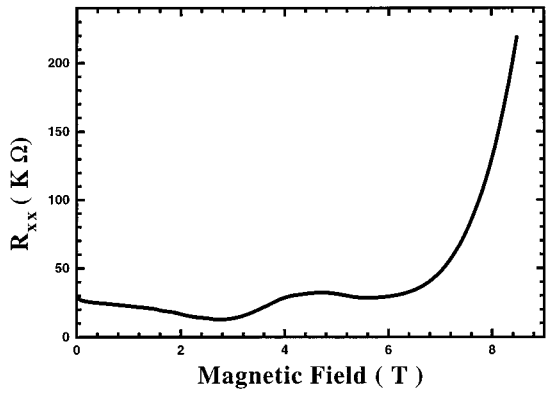

FIG. 10. R_{xx} as a function of the magnetic field after etching the quantum wells, but without removing the contacts. The figure shows that the oscillations are no longer present, confirming that our data on these samples before etching was taken in the quantum wells and not at the heterointerface.

wells with well widths ranging from about 30 Å to more than 100 Å. None of these conducted at or below 20 K, and no PPC was observed in any of them, in sharp contrast to what we observed in the $Ga_xIn_{1-x}P$/GaAs structures.

DX centers in doped $Al_xGa_{1-x}As$/GaAs structures are well studied and it is found that their concentration increases with the doping density. It is now well accepted that the DX centers are responsible for the PPC observed in doped $Al_xGa_{1-x}As$/GaAs materials. It was also found that, regardless of the concentration of dopants, no PPC is observed if the aluminum mole fraction is less than 0.2 (see Reference 21). In $Ga_xIn_{1-x}P$/GaAs, PPC is present in *both undoped and doped* structures. As stated earlier, it is found that the defect responsible for PPC in undoped $Ga_xIn_{1-x}P$ structures is suppressed by doping. So unlike the DX center, whose concentration increases with the dopant density, the center responsible for PPC in undoped $Ga_xIn_{1-x}P$ is suppressed by doping. This is particularly true for silicon-doped $Ga_xIn_{1-x}P$, where either no PPC, or an insignificant amount of PPC, is observed. Regardless of whether or not there is a DX center, the fact that we see PPC means that, initially, electrons in the barrier are prevented from falling into the well by a potential barrier whose height is larger than the available thermal energy. This barrier is easily overcome by photoexcited electrons. Once in the well, the photoexcited electrons are prevented from returning to their original location by a capture barrier (originating from band bending) whose height is much larger than the thermal energy at temperatures below 77 K.

III. INTERFACE ROUGHNESS

It is well known that at low temperatures, interface roughness scattering dominates the mobility of high density ($>10^{12}$ cm^{-2}) 2DEG's in metal-oxide-semiconductor (MOS) inversion layers.[32–34] However, it has been argued that this scattering mechanism plays a negligible role in heterojunctions, for two different reasons. First, with current crystal growth methods, high crystalline quality with atomically sharp resolution is easily achieved; that is, the interfaces are not especially rough. Second, because the electron confining potential (the triangular potential well) in a single heterojunction is weak, the electron system is not tightly constrained to the interface and will only be weakly affected by interface roughness. Impurity scattering is found to be the dominant scattering mechanism in these structures.[35] However, the situation is completely different for very thin quantum wells (QW's) since a small roughness at the interface can cause a large fluctuation in the quantization energy of the 2DEG. It is expected that these large fluctuations can lead to very strong scattering.[33]

Several authors have considered the effect of interface roughness on the properties of thin quantum wells. Gold[36] predicts that at low temperatures the dominant scattering mechanism in thin quantum wells is interface roughness. His calculations showed that interface-roughness-limited mobility, μ, depends very strongly on the well width (L), $\mu \propto L^6$, and only weakly on the carrier density. He also predicts a metal-insulator transition with thickness in thin $Al_xGa_{1-x}As$/GaAs/$Al_xGa_{1-x}As$ quantum wells due to electron localization induced by interface roughness scattering. He argues that this metal-insulator transition occurs when the well width decreases to a critical value L_c, which depends on the dominant scattering mechanism. For interface roughness, Gold estimated the value of L_c to be about 60 Å in $Al_xGa_{1-x}As$/GaAs/$Al_xGa_{1-x}As$ quantum wells. This dependence of the mobility on the well thickness was confirmed[37] in experiments on GaSb/InAs/GaSb quantum wells. Sakaki *et al.*[33] studied theoretically and experimentally the influence of interface roughness on the mobility of a 2DEG in modulation-doped AlAs/GaAs/AlAS quantum wells. They concluded that interface roughness scattering *is* the dominant scattering mechanism in thin quantum wells of this type when the well width $L<60$ Å, and that the interface-roughness-limited mobility is proportional to L^6. Gottinger *et al.*,[38] in a study of the mobility in 2DEG's in thin $Al_xGa_{1-x}As$/GaAs/$Al_xGa_{1-x}As$ quantum wells, report that a strong decrease in the mobility is found for well widths below 60 Å and they attribute this to interface roughness. However, they report observed mobilities much higher than those predicted by Gold's theory for an infinite barrier height.

We have tested if what has been predicted and observed in AlAs/GaAs/AlAs materials holds for GaInP/GaAs/GaInP structures. In such a measurement we would be able to test the influence of the barrier since the transport coefficients

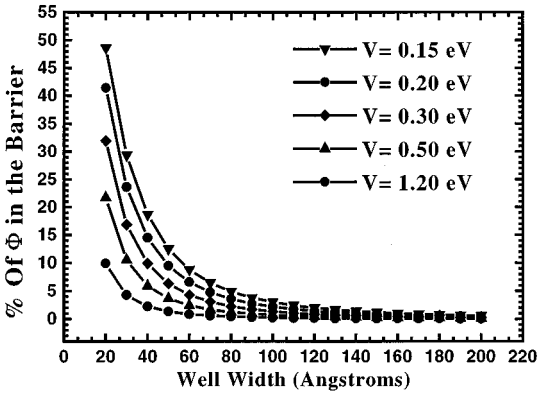

FIG. 11. The total probability of penetration of the wave function Φ into the barrier as a function of the well width. The points are calculated values and the lines are added to ease comparison.

TABLE II. This table shows how the mobility depends on the well width L for different structures. Shown here are the λ values ($\mu \alpha L^{\lambda}$) for different structures. SL denotes superlattice.

Material	ΔE_c (eV)	λ	Structure	Reference
AlSb/InAs	1.35	6	SQW	Bolognesi *et al.*[a]
CdTe/HgTe	1.14	6	SL	Meyer *et al.*[b]
AlAs/GaAs	1.2	6	SQW	Sakaki *et al.*[c]
$Al_xGa_{1-x}As$/GaAs	0.27	3.4	SQW	Gottinger *et al.*[d]
$Ga_xIn_{1-x}Sb$/InAs	0.1	2.4	SL	Hoffmann *et al.*[e]
$Ga_xIn_{1-x}P$/GaAs	0.2	1.3	SQW	This work

[a]Appl. Phys. Lett. **61**, 213 (1992).
[b]Appl. Phys. Lett. **58**, 2523 (1991).
[c]Appl. Phys. Lett. **51**, 1934 (1987).
[d]Europhys. Lett. **6**, 183 (1988).
[e]Appl. Phys. Lett. **63**, 2210 (1993).

measured in both structures are those of a 2DEG residing in the same material (GaAs). First, we extended Fig. 1 of Sakaki *et al.* (reproduced here as Fig. 9) to well widths of 20 and 25 Å, *using their parameters for interface roughness, which are suitable for AlAs/GaAs/AlAs*. From the figure, mobilities of approximately 10 and 25 cm^2/V sec are predicted for these wells for carrier concentrations in the low to mid 10^{11}-cm^{-2} range. We then plot the mobilities measured for our samples, as a function of their well width, along with those predicted from the results of Sakaki *et al.* in Fig. 9. We can see a large discrepancy between what is reported by Sakaki *et al.* and by Gold for $Al_xGa_{1-x}As$/AlGa/$Al_xGa_{1-x}As$ and what we observe in $Ga_xIn_{1-x}P$/AlGa/$Ga_xIn_{1-x}P$. A linear fit to our data shows a mobility that varies as $L^{1.3}$, very different from the L^6 dependence predicted by Sakaki *et al.* and Gold. Noda, Tanaka, and Sakaki[39] report on the concentration dependence of the mobility in narrow quantum wells. The concentration dependence of the mobilities in their 50-Å AlAs/GaAs/AlAs well at 4.2 K resembles the data in Fig. 8 in that the mobility is flat at the lowest concentrations and then increases rapidly with n. However, the lowest measured mobility in their sample, at a carrier concentration of 2×10^{11} cm^{-2}, was only 3000 cm^2/V sec, compared to the 10 000 cm^2/V sec we observe at a comparable concentration for our 20-Å well. The similarity between the shape of the two figures (the mobility versus concentration curve) suggests that we are observing interface-roughness-scattering-dominated transport in a narrow quantum well, but the magnitudes of the mobilities we measure appear to be too high. How can we reconcile these discrepancies?

Interface roughness is characterized by two parameters, the height Δ of the ''step'' in the interface and the lateral size Λ of that step. The calculations of Sakaki *et al.* for AlAs/GaAs/AlAs were made assuming an interface roughness step height between 1 and 3 ML and a lateral size between 50 and 70 Å. Based on their lateral size dependence of the mobility as a function of carrier density, we estimate the value for Λ for our samples to be at least 100 Å. We do not feel that it is reasonable to assume that the $Ga_{0.51}In_{0.49}P$/GaAs interfaces are perfectly smooth but an improvement of 1 to 2 ML for the step height, particularly on the inverted surface, is not unreasonable. Even that, however, does not appear to be enough to move the measured mobilities into the expected range. Since the theory appears to work for AlAs/GaAs/AlAs, it can only be concluded that material-related parameters, such as the barrier height, must be playing a more significant role than previously believed. We ruled out the possibility of our signal coming from the heterojunction (whose mobilities are usually higher than those of quantum wells) between the GaAs buffer layer and the bottom layer of $Ga_xIn_{1-x}P$. To do this, we etched away the quantum well without removing the contacts and remeasured R_{xx}. The results are shown in Fig. 10. The data demonstrate that the Shubnikov–de Haas oscillations are no longer present, confirming that the results on these samples before etching came from the quantum wells and not the heterointerface.

In their calculations, both Gold[36] and Sakaki *et al.*[33] assume an infinite barrier height. With this assumption, the wave function of an electron cannot penetrate into the barrier material. For finite barrier heights, however, the electron wave function does penetrate into the barrier and interface irregularities will cause weaker fluctuations in the confinement energies than for the infinite barrier: interface roughness scattering is weakened compared to a well with an infinite barrier height.[38] For silicon metal-oxide-semiconductor structures, the conduction-band offset between the silicon and silicon dioxide is about 3.14 eV.[32] In AlAs/GaAs/AlAs quantum wells the barrier height of the confining potential V is about 1.2 eV, whereas the confining potential in $Ga_xIn_{1-x}P$/GaAs/$Ga_xIn_{1-x}P$ is only 0.198 eV, an order of magnitude smaller. The effective confining potential for the electrons is going to be even smaller than 0.198 eV, especially if more than one subband is populated.

In a later publication, reporting on barrier penetration effects for electrons in quantum wells with finite barrier heights, Gold[40] argues that the mobility in narrow quantum wells with finite barrier height should be higher than that in wells of the same width but infinite barrier potential. For a finite confining potential, Gold shows that the width dependence of the mobility goes as $L^{(6-2d)}$ where the correction term d depends on the confining potential. For small confining potentials, Gold predicts that d could be >3.

To determine how much of the wave function penetrates into the barrier as a function of the well width, we plot in Fig. 11 the total probability of penetration of the wave func-

tion into the barrier as a function of the well width. The calculation assumes that carriers in the barrier and the host materials have the same effective mass and that the host material is GaAs. How much of the wave function penetrates into the barrier depends both on the well width and on the barrier height. For wide well widths ($L>100$ Å), the total penetration probability is less than 10% and is not very sensitive to the barrier height. For narrow well widths, the total probability of penetration into the barrier depends strongly on the confining potential. For a well width of 20 Å, the total probability of penetration into the barrier for $V=0.05$ eV is 75%, whereas that for $V=0.5$ eV is only 22%, a very significant difference. The calculations reflected in this graph confirm that barrier height plays a more important role in narrow quantum wells than it does in wide quantum wells.

In Table II, we summarize how the mobility depends on the well width $\mu \alpha L^{\lambda}$. We notice that the value of λ increases as the barrier height increases for a single quantum well (SQW). Our value of λ is the smallest reported value. This can adversely affect devices where confinement is important but does lead to significantly higher mobilities in narrow quantum wells such as in the samples studied here.

We conclude that finite confining potentials are responsible for both the high mobilities and their dependence on well width ($\mu \propto L^{(1.3)}$) of our samples. The finite barrier height allows the wave function to penetrate into the barrier, reducing the effects of interface roughness scattering. This is an important observation because it can adversely affect devices where confinement is important, but leads to significantly higher mobilities in narrow quantum wells.

*Permanent address: Physics Department, Xavier University, Cincinnati, OH 45207.

[1] M. Razeghi, P. Maurel, and F. Omnes, Appl. Phys Lett. **48**, 1267 (1986).
[2] A. Ginoudi, E. C. Paloura, G. Kostandinidis, G. Kirakidis, Ph. Maurel, J. C. Garcia, and A. Christou, Appl. Phys. Lett. **60**, 3162 (1992).
[3] Miyoko O. Watanabe and Yasuo Ohba, J. Appl. Phys. **60**, 1032 (1996).
[4] Kuninori Kitahara, Masataka Hoshino, Kunihiko Kodama, and Masashi Ozeki, Jpn. J. Appl. Phys. **25**, L534 (1986).
[5] Kuninori Kitahara, Masataka Hoshino, Kunihiko Kodama, and Masashi Ozeki, Jpn. J. Appl. Phys. **25**, L191 (1986).
[6] D. V. Lang and R. A. Logan, Phys. Rev. Lett. **39**, 635 (1977).
[7] D. V. Lang, R. A. Logan, and M. Jaros, Phys. Rev. B **19**, 1015 (1979).
[8] K. Tone, T. Nakayama, H. Iechi, K. Ohtsu, and H. Kukimoto, Jpn. J. Appl. Phys. **25**, L429 (1986).
[9] P. R. Hageman, A. van Geelen, W. Gabrielse, G. J. Bauhuis, and L. J. Giling, J. Cryst. Growth **125**, 336 (1992).
[10] J. M. Olson, R. K. Ahrenkiel, D. J. Dunlavy, Brian Keyes, and A. E. Kibbler, Appl. Phys. Lett. **55**, 1208 (1989).
[11] F. E. G. Guimaraes, B. Elsner, R. Westphalen, B. Spangenberg, H. J. Geelen, P. Balk, and K. Heime, J. Cryst. Growth **124**, 199 (1992).
[12] M. J. Matragrano, V. Krishnamoorthy, D. G. Ast, and J. R. Shealy, J. Cryst. Growth **142**, 275 (1994).
[13] E. C. Paloura, A. Ginoudi, G. Kiriakidis, and A. Christou, Appl. Phys. Lett. **59**, 3127 (1991).
[14] K. Kodama, M. Hoshino, K. Kitahara, M. Takikawa, and M. Ozeki, Jpn. J. Appl. Phys. **25**, L127 (1986).
[15] D. Biswas, N. Debbar, P. Bhattacharya, M. Razeghi, M. Defour, and F. Omnes, Appl. Phys. Lett. **56**, 833 (1990).
[16] Kiyoshi Tone, Takao Nakayama, Hiroyuki Iechi, Kazuyoshi Ohtsu, and Hiroshi Kukimoto, Jpn. J. Appl. Phys. **25**, L429 (1986).
[17] K. Kodama, M. Hoshino, K. Kitahara, M. Takikawa, and M. Ozeki, Jpn. J. Appl. Phys. **25**, L127 (1986).
[18] E. Ranz, D. Lavielle, L. A. Cury, J. C. Portal, M. Razeghi, and F. Ommes, Superlatt. Microstruct. **8**, 245 (1990).
[19] Z. P. Jiang, P. B. Fisher, S. Y. Chou, and M. I. Nathan, J. Appl. Phys. **71**, 4632 (1992).
[20] M. R. Reed, W. P. Kirk, and P. S. Kobiela, IEEE J. Quantum Electron. **QE-22**, 175 (1986).
[21] P. M. Mooney, J. Appl. Phys. **67**, R1 (1990).
[22] M. Razeghi, M. Defour, F. Omnes, M. Dobers, J. P. Vieren, and Y. Guldner, Appl. Phys. Lett. **55**, 457 (1989).
[23] S. Ben Amor, L. Dmowski, J. C. Portal, N. J. Pulsford, R. J. Nicholas, J. Singleton, and M. Razeghi, J. Appl. Phys. **65**, 2756 (1989).
[24] S. L. Feng, J. C. Bourgoin, F. Omnes, and M. Razeghi, Appl. Phys. Lett. **59**, 941 (1991).
[25] J. Krynicki, M. A. Zaide, M. Zazoui, J. C. Bourgoin, M. DiForte-Poisson, C. Brylinski, S. L. Delage, and M. Blank, J. Appl. Phys. **74**, 260(1993).
[26] J. B. Lee, S. D. Kwon, Y. H. Cho, and B. D. Choc, J. Appl. Phys. **71**, 5016 (1992).
[27] S. Elhamri, M. Ahoujja, K. Ravindran, D. B. Mast, R. S. Newrock, W. C. Mitchel, G. J. Brown, I. Lo, M. Razeghi, and Xiaguang He, Appl. Phys. Lett. **66**, 171 (1995).
[28] I. Lo, W. C. Mitchel, M. O. Manasreh, C. E. Stutz, and K. R. Evans, Appl. Phys. Lett. **60**, 751 (1992).
[29] R. G. Mani and J. R. Anderson, Phys. Rev. B **37**, 4299 (1988).
[30] F. F. Fang, A. B. Fowler, and A. Hartstein, Phys. Rev. B **16**, 4446 (1977).
[31] S. Das Sarma and F. Stern, Phys. Rev. B **32**, 8442 (1985).
[32] T. Ando, A. B. Fowler, and F. Stern, Rev. Mod. Phys. **54**, 437 (1982).
[33] H. Sakaki, T. Noda, K. Hirakawa, M. Tanaka, and T. Matsusue, Appl. Phys. Lett. **51**, 1934 (1987).
[34] H. Harstein, T. H. Ning, and A. B. Fowler, Surf. Sci. **58**, 178 (1976).
[35] T. Ando, J. Phys. Soc. Jpn. **51**, 3900 (1982).
[36] A. Gold, Solid State Commun. **60**, 531 (1986).
[37] H. Munekata, E. E. Mendez, Y. Iye, and L. Esaki, Surf. Sci. **174**, 449 (1986).
[38] R. Gottinger, A. Gold, G. Abstreiter, and G. Weilmann, Europhys. Lett. **6**, 183 (1988).
[39] T. Noda, M. Tanaka, and H. Sakaki, Appl. Phys. Lett. **57**, 1651 (1990).
[40] A. Gold, Z. Phys. B **74**, 53 (1989).